CONSTRAINED DIFFERENTIAL EQUATIONS AS COMPLEX SOUND GENERATORS

Dario SANFILIPPO[1]

[1]**Independent**, Catania, Italy

ABSTRACT

This paper presents investigations for complex sound generation based on modified classic chaotic differential equations. The modification consists of a constraining structure, a cascaded saturating nonlinearity and DC-blocker unit within the recursive paths of the differential equations. The new configuration allows for the exploration of these equations in unstable regions, increasing the parameters ranges allowed and extending sonic possibilities. Furthermore, the configuration implements a low-level competing mechanism between positive and negative feedback relations that forces oscillation and enhances complex variations both at timbral and formal time scales. The resulting systems exhibit phase spaces with nontrivial trajectories and show potential for computer music and, particularly, applications requiring some degree of autonomy. The sound generators are implemented in the Faust programming language and are published on Github under the GNU GPL v3.0 license.

1. INTRODUCTION

Differential equations exhibiting chaotic behaviours have been studied for over a century and have found applications in several fields ranging from biology and chemistry to electronics and mechanics. The Lotka-Volterra equations are a system of two differential equations conceived in the 1910s and used to this day to model biological systems, particularly predator-prey interactions and dynamics [1]. The Duffing equation is a second-order differential equation and was initially investigated in the late 1910s to render the behaviour of particular damped oscillators [2]. In the 1920s, Balthasar van der Pol discovered a differential equation for a type of stable oscillator connected to behaviours in electrical circuits applying vacuum tubes [3]. The Lorenz system is a system of three differential equations developed in the 1960s as a mathematical model for atmospheric convection; the system later became one of the most iconic models displaying deterministic chaos [4]. Later, in the 1970s, Otto Rössler designed a chaotic attractor initially intended to behave similarly to the Lorenz attractor that was later found to be related to equilibrium in chemical reactions [5]. The Chua's circuit, developed in the 1980s, is an electrical circuit exhibiting chaotic behaviours that can be modelled through a system of three differential equations and that became famous for its simplicity of construction [6]. Also in the 1980s, Hindmarsh and Rose produced a system of three differential equations to model neuronal activity [7]. Lastly, in the 1990s, René Thomas developed a system of three differential equations that could be used to model a particle's motion in a 3D lattice of forces [8].

Early examples of the application of chaotic systems for music date back to the late 1990s with Di Scipio's work on iterated nonlinear functions [9, 10]. There, Di Scipio investigates difference equations based on the sine map model for the generation of spectrally rich synthetic sounds and dynamical behaviours and simulations of auditory environmental events. In the 2000s, we have investigations by Bilotta et al., where the Chua oscillator is explored extensively for musical and artistic applications [11, 12]. More recent works on musical applications of chaotic systems can be found in [13] and [14]. Mudd, in particular, develops a form of modified Duffing equation where the dynamics of the system is guided through a band-pass filter bank; the equation and the filters are coupled through an added outer feedback loop. Finally, a survey of feedback-based music describing several approaches that can all be grouped within the realm of nonlinear iterated functions is available in [15].

Since Bilotta et al. and Mudd have carried out research on Chua's circuit and Duffing equation, in the next section, we will focus on the remaining differential equations mentioned earlier: Lotka-Volterra, van der Pol, Lorenz, Rössler, Hindmarsh-Rose, and Thomas.

2. COMPLEX SOUND GENERATORS

This section will discuss the implementation of complex sound generators based on modified chaotic differential equations, and we will present results to show their musical potential.

Considering first-order differential equations, we can obtain a generalisation of the modified systems discussed here. Let y be a vector of functions, let x be an input vector, let F be a vector of functions of y and x; let C be a vector of constraining functions. Written in differential form with respect to time, we have that:

$$\frac{\partial y(t)}{\partial t} = C(F(x(t), y(t))) \quad (1)$$

where

$$C(z) = B(l \cdot S(z/l)) \tag{2}$$

with B and S being, respectively, vectors of first-order DC-blockers and saturating nonlinearities with arbitrary saturation threshold piloted by the parameter l. The saturation threshold becomes a key parameter for the interaction with the oscillators, while the overall output can be normalised to unity peak amplitudes for digital audio by merely dividing by l. While several types of bounded saturators are available [16], here, we will focus on the well-known hyperbolic tangent function. Note that the input vector can be used to set the system's initial conditions or as continuous perturbation through signals. In fact, these systems can also be deployed as nonlinear distortion units when operating under non-self-oscillating conditions.

The working concept for the constraining function is inherent to the nature of the differential equations studied here. Firstly, tendencies towards fixed-point attractors [17] will be counteracted by the DC-blockers, which will result in self-oscillating behaviours due to mutually compensating mechanisms. Secondly, tendencies towards unbounded exponential growth will be turned into fixed-points by the saturating functions, which will subsequently be contrasted by the DC-blocker, favouring self-oscillation and evolutions at timbral and formal time scales. The resulting modified systems are structurally stable for any parameters values and can be explored through a larger state variable space. Visual phase space analysis [18, 19] shows novel and enhanced complex behaviours. Note that while the DC-blockers have a fixed cut-off of ten Hz for the examples below, their frequency, when using sub-audio cut-off values, can be a key parameter for formal-level variations. In particular, the parameter sets the responsiveness for the fixed-point counterbalancing mechanism.

The differential equations and their respective discretised models will be shown later. The implementation of the generators in the Faust [1] language is available on `http://github.com/dariosanfilippo`. Audio examples are available on `http://soundcloud.com/dario-sanfilippo`.

2.1 Remarks on nonlinearities and aliasing distortion

Aliasing distortion is a common problem in digital audio, and it can significantly compromise the quality of computer-generated sound and music. For example, several techniques have been developed to overcome issues related to aliasing in digital oscillators of classic analogue waveforms [20–22]. Processing audio signals through nonlinearities, too, can result in high aliasing distortion depending on the nature of the process. Particularly for saturators such as the hyperbolic tangent function, we have the generation of odd harmonics given by the odd symmetry of the function, while their strength is proportional to the amplitude of the input signal. A standard technique to counterbalance aliasing distortion, in general, is oversampling, while more efficient techniques based on antiderivatives have been explicitly developed for nonlinear processing [23–25].

Unlike aliasing distortion in digital oscillators or saturators used in feedforward configurations, aliasing distortion in recursive systems such as those discussed here acquires a systemic role within global behaviours and has proven to be worthy of exploration for musical purposes. Nonetheless, applications of antialiasing techniques will be investigated in the future to realise more accurate approximations of the models in this paper. The author already operates these systems at 192 kHz sample-rate to reduce distortion – a low-order oversampling ratio achievable on most hardware devices when oversampling is not available via software.

2.2 Discrete models

For the discretisation of continuous-time systems, we will rely on the Euler method for first-order approximation [26]. For simplicity, the discrete equations will only include approximations of the continuous differential equations and omit the input signals and the constraining functions showed in (1) and implemented in the Faust code. Note that to clarify the discretisation, the dimensions of the systems were named after the original differential equations rather than following the general formula (1). The numerical simulations below are in double-precision; the parameters were chosen according to trial-and-error processes.

2.2.1 Lotka-Volterra

The Lotka-Volterra system consists of two differential equations with four parameters. The equations model biological systems and interaction dynamics between predator-prey couples. The four parameters, assumed to be positive real values, govern critical aspects of a biological system such as the population growth of preys and predators and the degree of interaction between the two:

$$\begin{aligned} \frac{\partial x}{\partial t} &= \alpha x - \beta xy \\ \frac{\partial y}{\partial t} &= \delta xy - \gamma y \end{aligned} \quad . \tag{3}$$

The discrete model approximation is given by:

$$\begin{aligned} x[n] &= x[n-1] + \partial t(\alpha x[n-1] - \beta x[n-1]y[n-1]) \\ y[n] &= y[n-1] + \partial t(\delta x[n-1]y[n-1] - \gamma y[n-1]) \end{aligned} \tag{4}$$

where ∂t is the integration step.

Stability analysis and characteristics of Lotka-Volterra systems have been investigated largely. A notable publication describing global behaviours can be found in [27]. Be-

[1] `http://faust.grame.fr`

low, we can see the output of the modified Lotka-Volterra equations using parameters in unstable regions. Specifically, the parameters for this example are: $\alpha = 4$, $\beta = 1$, $\delta = 2$, and $\gamma = 1$, with the initial conditions set to 1 for both equations. The saturation threshold is 30, and the integration step, ∂t, is .1. In the non-modified equations, these parameters would result in an unbounded exponential growth that would exceed representability in floating-point double-precision after a few iterations.

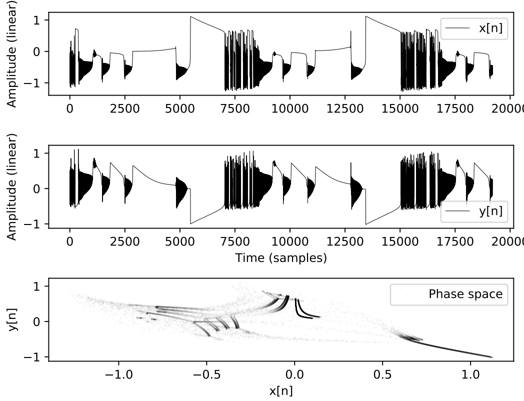

Figure 1. Modified Lotka-Volterra system outputs and phase space with $x_0 = 1$, $y_0 = 1$, $\alpha = 4$, $\beta = 1$, $\delta = 2$, $\gamma = 1$, $l = 30$, and $\partial t = .1$.

2.2.2 *Van der Pol*

The van der Pol system is a second-order differential equation describing a non-conservative oscillator with single nonlinear damping parameter. Dutch engineer Balthasar van der Pol discovered the system in the 1920s and found out that, under specific conditions, the oscillator would exhibit chaotic behaviours. The differential equation for the oscillator is:

$$\frac{\partial^2 x}{\partial t^2} - \mu(1 - x^2)\frac{\partial x}{\partial t} + x = 0 \quad , \tag{5}$$

where $\mu > 0$ represents the strength of the nonlinearity. Using Liénard's transformation [28]

$$y = x - \frac{x^3}{3} - \frac{\partial x}{\partial t}\frac{1}{\mu} \quad , \tag{6}$$

we can rewrite the Van der Pol second-order equation as a two-dimensional, first-order system as follows:

$$\begin{aligned} \frac{\partial x}{\partial t} &= \mu\left(x - \frac{x^3}{3} - y\right) \\ \frac{\partial y}{\partial t} &= \frac{x}{\mu} \end{aligned} \quad . \tag{7}$$

The discrete model for the Van der Pol oscillator is then:

$$\begin{aligned} x[n] &= x[n-1] + \\ &\partial t\left(\mu\left(x[n-1] - \frac{x^3[n-1]}{3} - y[n-1]\right)\right) \quad . \\ y[n] &= y[n-1] + \partial t\left(\frac{x[n-1]}{\mu}\right) \end{aligned} \tag{8}$$

In figure 2, we can see the response the system with constant input signals equal to 1, $l = 1.5733$, $\partial t = .904001$, and $\mu = .664$.

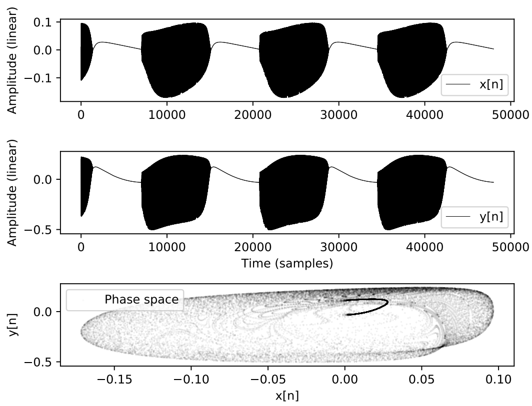

Figure 2. Modified Van der Pol system outputs and phase space with constant input signals equal to 1, $l = 1.5733$, $\partial t = .904001$, and $\mu = .664$.

2.2.3 *Lorenz*

The Lorenz system is one of the most influential models for deterministic chaos. It was initially developed in the 1960s by Edward Lorenz as a simplified model for atmospheric convection. The model is a first-order system of three differential equations relating convection to horizontal and vertical temperature variations [29]. The parameters σ, ρ, and β govern the relationships between the quantities. Lorenz initially chose the values $\sigma = 10$, $\rho = 8/3$, and $\beta = 28$, a parameters region displaying chaotic behaviours and producing the popular butterfly-like phase space. The system is given by:

$$\begin{aligned} \frac{\partial x}{\partial t} &= \sigma(y - x) \\ \frac{\partial y}{\partial t} &= x(\rho - z) - y \quad . \\ \frac{\partial z}{\partial t} &= xy - \beta z \end{aligned} \tag{9}$$

The discrete model is given by:

$$
\begin{aligned}
x[n] &= x[n-1] + \partial t(\sigma(y[n-1] - x[n-1])) \\
y[n] &= y[n-1] + \\
&\quad \partial t(x[n-1](\rho - z[n-1]) - y[n-1]) \\
z[n] &= z[n-1] + \partial t(x[n-1]y[n-1] - \beta z[n-1])
\end{aligned}
\quad . \tag{10}
$$

Dynamical behaviours of the Lorenz system are often investigated by keeping σ and ρ fixed to the values originally proposed by Lorenz while varying β in a range between 0 and 30 [30]. In the example showed in figures 3 and 4, we can see chaotic behaviours with $\sigma = 10$, $\rho = 2.67$, and $\beta = -10$. The integration step, ∂t, is set to 0.022001, and the saturation limit is $l = 143.810806$.

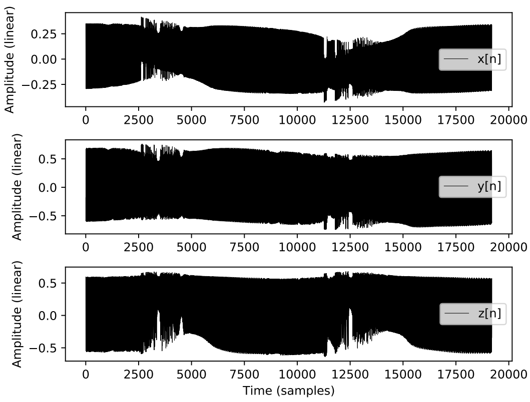

Figure 3. Modified Lorenz system impulse response outputs with $\sigma = 10$, $\rho = 2.67$, and $\beta = -10$. The integration step, ∂t, is set to 0.022001, and the saturation limit is $l = 143.810806$.

2.2.4 *Rössler*

The Rössler system was developed in the 1970s as a simplified model for continuous chaos with similar properties to those of the Lorenz system. Based on the Poincaré-Bendixson theorem for which a three-dimensional manifold is a minimum requirement for chaos, Rössler developed a first-order system of three differential equations with three parameters and minimal nonlinearity inspired by the geometry of relaxation-type systems [31]:

$$
\begin{aligned}
\frac{\partial x}{\partial t} &= -y - z \\
\frac{\partial y}{\partial t} &= x + ay \\
\frac{\partial z}{\partial t} &= bx - cz + xz
\end{aligned}
\quad . \tag{11}
$$

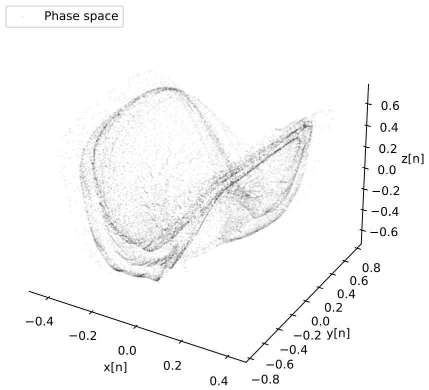

Figure 4. Modified Lorenz system impulse response phase space with $\sigma = 10$, $\rho = 2.67$, and $\beta = -10$. The integration step, ∂t, is set to 0.022001, and the saturation limit is $l = 143.810806$.

An example of chaotic behaviour is with the parameters $a = 0.38$, $b = 0.3$, and $c = 4.820$. The discrete model is given by:

$$
\begin{aligned}
x[n] &= x[n-1] + \partial t(-y[n-1] - z[n-1]) \\
y[n] &= y[n-1] + \partial t(x[n-1] + ay[n-1]) \\
z[n] &= z[n-1] + \\
&\quad \partial t(bx[n-1] - cz[n-1] + x[n-1]z[n-1])
\end{aligned}
\quad . \tag{12}
$$

In figures 5 and 6, we can see chaotic behaviours of the modified system through its outputs and phase space for $a = 0.776$, $b = 2.524$, $c = 13.98$, $\partial t = 2.075001$, and $l = 21.2554$.

2.2.5 *Hindmarsh-Rose*

The Hindmarsh-Rose system was developed in the 1980s as a model describing neuronal activity to study the behaviours of the membrane potential. Real neurons exhibit various behaviours ranging from quiescence to regular and irregular spiking-bursting outputs, and analysis of the model has shown that it can reproduce such behaviours correctly [32]. The model consists of three first-order differential equations and has eight parameters in total:

$$
\begin{aligned}
\frac{\partial x}{\partial t} &= y + \phi(x) - z + I \\
\frac{\partial y}{\partial t} &= \psi(x) - y \\
\frac{\partial z}{\partial t} &= r(s(x - x_R) - z)
\end{aligned}
\tag{13}
$$

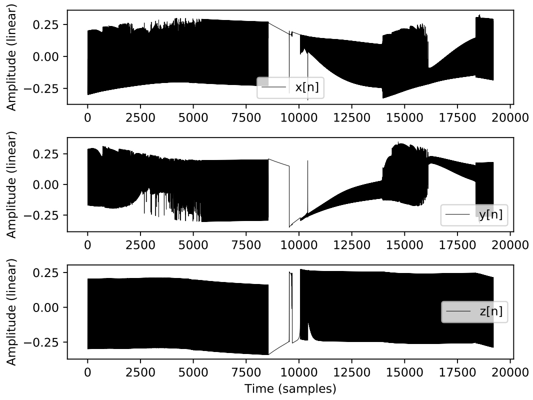

Figure 5. Modified Rössler system outputs for $a = 0.776$, $b = 2.524$, $c = 13.98$, $\partial t = 2.075001$, and $l = 21.2554$.

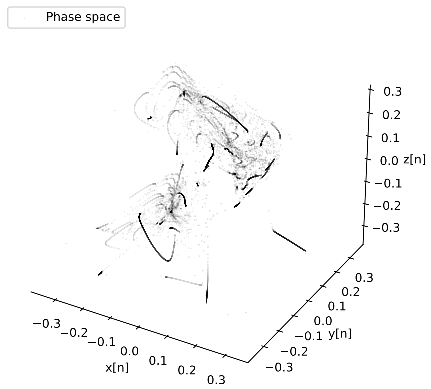

Figure 6. Modified Rössler system phase space for $a = 0.776$, $b = 2.524$, $c = 13.98$, $\partial t = 2.075001$, and $l = 21.2554$.

where

$$\begin{aligned} \phi(x) &= -ax^3 + bx^2 \\ \psi(x) &= c - dx^2 \end{aligned} \quad . \tag{14}$$

The discrete equations are:

$$\begin{aligned} x[n] &= x[n-1] + \\ &\quad \partial t(y[n-1] + \phi(x[n-1]) - z[n-1] + I) \\ y[n] &= y[n-1] + \partial t(\psi(x[n-1]) - y[n-1]) \\ z[n] &= z[n-1] + \partial t(r(s(x[n-1] - x_R) - z[n-1])) \end{aligned} \quad . \tag{15}$$

The neuronal model is often analysed by keeping some of the parameters fixed while varying the remaining ones. In [33], we have $a = 1$, $b = 3$, $c = -3$, $d = 5$, $s = 4$, and $I = 5$. In [34], instead, we have $a = 1$, $b = 3$, $c = 1$, $d = 5$, $s = 4$, and $x_R = 8/5$, where chaotic regions are characterised in terms of Lyapunov analysis with positive peaks in the Lyapunov exponent being detected for $r = .0021$ and $I \approx 3.295$. In the examples of the modified Hindmarsh-Rose system, we will choose different parameters to show chaotic behaviours in alternative regions. In figures 7 and 8, we can see the outputs and phase space of the modified Hindmarsh-Rose model with $a = 1$, $b = -5.864$, $c = -20$, $d = -5.656$, $r = -.192$, $s = 3.104$, $I = -6.836$, and $x_R = 8.792$, with $l = 5.3989$ and $\partial t = .299001$.

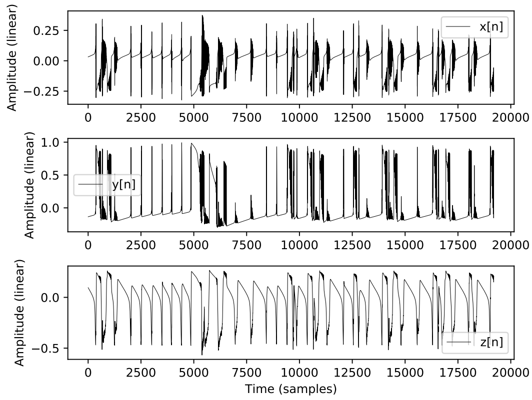

Figure 7. Modified Hindmarsh-Rose system phase space with $a = 1$, $b = -5.864$, $c = -20$, $d = -5.656$, $r = -.192$, $s = 3.104$, $I = -6.836$, and $x_R = 8.792$, with $l = 5.3989$ and $\partial t = .299001$.

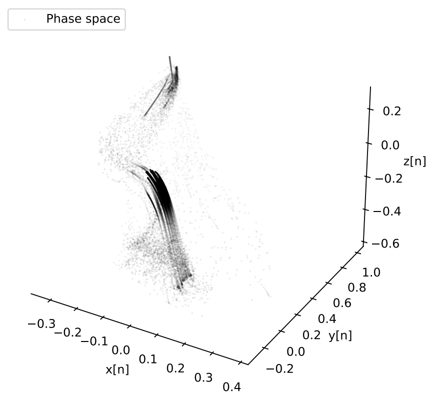

Figure 8. Modified Hindmarsh-Rose system phase space with $a = 1$, $b = -5.864$, $c = -20$, $d = -5.656$, $r = -.192$, $s = 3.104$, $I = -6.836$, and $x_R = 8.792$, with $l = 5.3989$ and $\partial t = .299001$.

2.2.6 Thomas

The Thomas system was developed in the late 1990s by René Thomas. It is a relatively simple three-dimensional first-order differential equation with one parameter representing damped particles moving in a 3D lattive of forces [35]. The system is defined by the following equations:

$$\begin{aligned}\frac{\partial x}{\partial t} &= \sin(y) - bx \\ \frac{\partial y}{\partial t} &= \sin(z) - by \\ \frac{\partial z}{\partial t} &= \sin(x) - bz\end{aligned} \quad . \tag{16}$$

The discrete model is given by:

$$\begin{aligned}x[n] &= x[n-1] + \partial t(\sin(y[n-1]) - bx[n-1]) \\ y[n] &= y[n-1] + \partial t(\sin(z[n-1]) - by[n-1]) \\ z[n] &= z[n-1] + \partial t(\sin(x[n-1]) - bz[n-1])\end{aligned} \quad . \tag{17}$$

In figures 9 and 10, we can see low-level and high-level complex oscillations with $b = .008$, $l = 5.3989$, and $\partial t = .841001$.

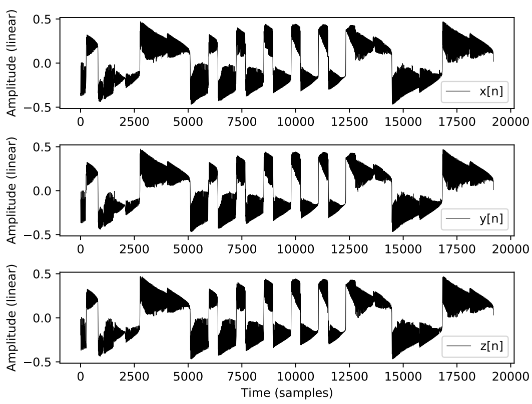

Figure 9. Modified Thomas system outputs with $b = .008$, $l = 5.3989$, and $\partial t = .841001$.

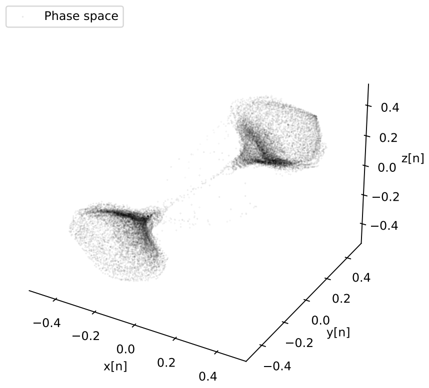

Figure 10. Modified Thomas system phase space with $b = .008$, $l = 5.3989$, and $\partial t = .841001$.

3. CONCLUSION

In this paper, we have discussed the investigation of modified differential equations to generate complex audio signals for musical applications. While the original differential equations studied here provided complex behaviours for specific configurations of the parameters, those systems only allowed for a limited state variable exploration due to possible stability issues. The modified equations proposed here deploy a constraining mechanism based on cascaded saturating nonlinearities and DC-blocking units that make the systems structurally stable and produce output signals in ranges suitable for digital audio applications. Most importantly, the constraining mechanism provides a low-level configuration establishing an interplay between positive and negative feedback relations, which results in nontrivial dynamical behaviours at timbral and formal time scales. The modified systems can be explored through a larger state variable for novel and enhanced complex sound generation and can be deployed in computer music environments in general and, more specifically, human-machine interaction performances requiring agency and autonomy as discussed in [36, 37].

Future works include applying higher-order methods for the solution of differential equations [38] and antialiased nonlinearities as discussed in 2.1 for a better approximation of the models, and advanced adaptation techniques for time-variant generators with increased complexity following [39–41]. Taking advantage of the implementation that allows for input signals to be used as external perturbation, the individual systems can be combined into networks of interacting components to explore emergent behaviours resulting from their synergy.

Finally, an extension of this work will be an analytical examination and comparison between the classic chaotic differential equations and the proposed modified systems. By means of Lyapunov exponent analysis [42], it will be possible to determine the effects of the constraining infrastructures concerning the sensitivity to initial conditions of the systems, while phase space analysis using musically-relevant dimensions such loudness, spectral centroid, and noisiness can provide a tool for the comparison of higher-level complexity in the original and modified systems.

4. REFERENCES

[1] A. J. Lotka, "Contribution to the theory of periodic reactions," *The Journal of Physical Chemistry*, vol. 14, no. 3, pp. 271–274, 2002.

[2] G. Duffing, *Erzwungene Schwingungen bei veränder-*

licher Eigenfrequenz und ihre technische Bedeutung. Vieweg, 1918, no. 41-42.

[3] B. Van der Pol, "Lxxxviii. on "relaxation-oscillations"," *The London, Edinburgh, and Dublin Philosophical Magazine and Journal of Science*, vol. 2, no. 11, pp. 978–992, 1926.

[4] E. N. Lorenz, "Deterministic nonperiodic flow," *Journal of atmospheric sciences*, vol. 20, no. 2, pp. 130–141, 1963.

[5] O. E. Rössler, "An equation for continuous chaos," *Physics Letters A*, vol. 57, no. 5, pp. 397–398, 1976.

[6] T. Matsumoto, "A chaotic attractor from chua's circuit," *IEEE Transactions on Circuits and Systems*, vol. 31, no. 12, pp. 1055–1058, 1984.

[7] J. L. Hindmarsh and R. Rose, "A model of neuronal bursting using three coupled first order differential equations," *Proceedings of the Royal society of London. Series B. Biological sciences*, vol. 221, no. 1222, pp. 87–102, 1984.

[8] R. Thomas, "Deterministic chaos seen in terms of feedback circuits: Analysis, synthesis," labyrinth chaos"," *International Journal of Bifurcation and Chaos*, vol. 9, no. 10, pp. 1889–1905, 1999.

[9] A. Di Scipio and I. Prignano, "Synthesis by functional iterations. a revitalization of nonstandard synthesis," *Journal of New Music Research*, vol. 25, no. 1, pp. 31–46, 1996.

[10] A. Di Scipio, "Synthesis of environmental sound textures by iterated nonlinear functions," in *Proceedings of the 2nd COST G-6 Workshop on Digital Audio Effects (DAFx99)*, 1999, pp. 109–117.

[11] E. Bilotta and P. Pantano, "The language of chaos," *International Journal of Bifurcation and Chaos*, vol. 16, no. 03, pp. 523–557, 2006.

[12] ——, *Gallery Of Chua Attractors, A (With Dvd-rom)*. World Scientific, 2008, vol. 61.

[13] T. Clutterbuck, T. Mudd, and D. Sanfilippo, "A practical and theoretical introduction to chaotic musical systems," in *In Proc. of the International Conference on Live Interfaces, eds. Thor Magnusson, Chris Kiefer, and Sam Duffy.*, 2016.

[14] T. Mudd, "Between chaotic synthesis and physical modelling: Instrumentalising with gutter synthesis," in *Procedings of the Conference on Compuation, Communication, Aesthetics and X (xCoAx)*, 2019, pp. 217–228.

[15] D. Sanfilippo and A. Valle, "Feedback systems: An analytical framework," *Computer Music Journal*, vol. 37, no. 2, pp. 12–27, 2013.

[16] V. Zavalishin, "The art of va filter design," *Native Instruments, Berlin, Germany*, 2012.

[17] J. Gleick, *Chaos: Making a new science*. Open Road Media, 2011.

[18] D. D. Nolte, "The tangled tale of phase space," *Physics today*, vol. 63, no. 4, pp. 33–38, 2010.

[19] H. Sayama, *Introduction to the modeling and analysis of complex systems*. Open SUNY Textbooks, 2015.

[20] T. Stilson and J. O. Smith III, "Alias-free digital synthesis of classic analog waveforms," in *ICMC*, 1996.

[21] J. Nam, V. Valimaki, J. S. Abel, and J. O. Smith, "Efficient antialiasing oscillator algorithms using low-order fractional delay filters," *IEEE transactions on audio, speech, and language processing*, vol. 18, no. 4, pp. 773–785, 2009.

[22] V. Valimaki, J. Nam, J. O. Smith, and J. S. Abel, "Alias-suppressed oscillators based on differentiated polynomial waveforms," *IEEE Transactions on audio, speech, and language processing*, vol. 18, no. 4, pp. 786–798, 2009.

[23] J. D. Parker, V. Zavalishin, and E. Le Bivic, "Reducing the aliasing of nonlinear waveshaping using continuous-time convolution," in *Proc. Int. Conf. Digital Audio Effects (DAFx-16), Brno, Czech Republic*, 2016, pp. 137–144.

[24] S. Bilbao, F. Esqueda, J. D. Parker, and V. Välimäki, "Antiderivative antialiasing for memoryless nonlinearities," *IEEE Signal Processing Letters*, vol. 24, no. 7, pp. 1049–1053, 2017.

[25] M. Holters, "Antiderivative antialiasing for stateful systems," *Applied Sciences*, vol. 10, no. 1, p. 20, 2020.

[26] S. Bilbao, *Numerical sound synthesis: finite difference schemes and simulation in musical acoustics*. John Wiley & Sons, 2009.

[27] Y. Takeuchi, *Global dynamical properties of Lotka-Volterra systems*. World Scientific, 1996.

[28] D. Kaplan and L. Glass, *Understanding nonlinear dynamics*. Springer Science & Business Media, 1997.

[29] C. Sparrow, *The Lorenz equations: bifurcations, chaos, and strange attractors*. Springer Science & Business Media, 2012, vol. 41.

[30] W. Song and J. Liang, "Difference equation of lorenz system," *International Journal of Pure and Applied Mathematics*, vol. 83, no. 1, pp. 101–110, 2013.

[31] P. Gaspard, "Rössler systems," *Encyclopedia of nonlinear science*, vol. 231, pp. 808–811, 2005.

[32] M. Storace, D. Linaro, and E. de Lange, "The hindmarsh–rose neuron model: bifurcation analysis and piecewise-linear approximations," *Chaos: An Interdisciplinary Journal of Nonlinear Science*, vol. 18, no. 3, p. 033128, 2008.

[33] A. Shilnikov and M. Kolomiets, “Methods of the qualitative theory for the hindmarsh–rose model: A case study–a tutorial,” *International Journal of Bifurcation and chaos*, vol. 18, no. 08, pp. 2141–2168, 2008.

[34] X.-J. Wang, “Genesis of bursting oscillations in the hindmarsh-rose model and homoclinicity to a chaotic saddle,” *Physica D: Nonlinear Phenomena*, vol. 62, no. 1-4, pp. 263–274, 1993.

[35] J. C. Sprott and K. E. Chlouverakis, “Labyrinth chaos,” *International Journal of Bifurcation and Chaos*, vol. 17, no. 06, pp. 2097–2108, 2007.

[36] D. Sanfilippo and A. Di Scipio, “Environment-mediated coupling of autonomous sound-generating systems in live performance: An overview of the machine milieu project,” in *Proceedings of the 14th Sound and Music Computing Conference, Espoo, Finland*, 2017, pp. 5–8.

[37] A. Di Scipio and D. Sanfilippo, “Defining ecosystemic agency in live performance,” *Array*, pp. 28–43, 2019.

[38] D. Medine, “Dynamical systems for audio synthesis: Embracing nonlinearities and delay-free loops,” *Applied Sciences*, vol. 6, no. 5, p. 134, 2016.

[39] D. Sanfilippo, “Time-variant infrastructures and dynamical adaptivity for higher degrees of complexity in autonomous music feedback systems: the Order from Noise (2017) project,” *Musica/Tecnologia*, vol. 12, no. 1, pp. 119–129, 2018.

[40] ——, “Time-domain algorithms for low-level and high-level information processing,” *Computer Music Journal (pending peer-review)*, 2021.

[41] ——, “Complex adaptation in audio feedback networks for the synthesis of music and sounds,” *Computer Music Journal (pending peer-review)*, 2021.

[42] J. B. Dingwell, “Lyapunov exponents,” *Wiley encyclopedia of biomedical engineering*, 2006.